Chapter 7

Infrared Astronomy

A.T. Tokunaga

7.1 USEFUL EQUATIONS; UNITS

The Planck function in wavelength units ($\lambda_{\mu\mathrm{m}}$ in μm; T in K) is

$$\begin{aligned} B_\lambda &= 2hc^2\lambda^{-5}/(e^{hc/k\lambda T} - 1) \\ &= 1.191\,0 \times 10^8 \lambda_{\mu\mathrm{m}}^{-5}/(e^{14\,387.7/\lambda_{\mu\mathrm{m}}T} - 1)\ \mathrm{W\,m^{-2}\,\mu m^{-1}\,sr^{-1}}. \end{aligned}$$

The Planck function in frequency units (ν in Hz) is

$$\begin{aligned} B_\nu &= 2h\nu^3c^{-2}/(e^{h\nu/kT} - 1) \\ &= 1.474\,5 \times 10^{-50}\nu^3/(e^{4.799\,22\times10^{-11}\,\nu/T} - 1)\ \mathrm{W\,m^{-2}\,Hz^{-1}\,sr^{-1}}. \end{aligned}$$

The Rayleigh–Jeans approximation (for $h\nu \ll kT$) is

$$B_\lambda = 2ckT\lambda^{-4} = 8.278\,2 \times 10^3\ T/\lambda^4_{\mu\text{m}}\ \text{W m}^{-2}\,\mu\text{m}^{-1}\,\text{sr}^{-1},$$
$$B_\nu = 2c^{-2}kT\nu^2 = 3.072\,4 \times 10^{-40}\ T\nu^2\ \text{W m}^{-2}\,\text{Hz}^{-1}\,\text{sr}^{-1}.$$

The Stefan–Boltzmann law is

$$B = \int B_\lambda\, d\lambda = (\sigma/\pi)T^4 = 1.805\,0 \times 10^{-8}\ T^4\ \text{W m}^{-2}\,\text{sr}^{-1}.$$

The wavelength of maximum B_λ (Wien law) is

$$\lambda_{\text{max}} = 2\,898/T, \qquad \lambda_{\text{max}} \text{ in } \mu\text{m}.$$

The frequency of maximum B_ν is

$$\nu_{\text{max}} = 5.878 \times 10^{10}\ T, \quad \nu_{\text{max}} \text{ in Hz}.$$

The conversion equations (Ω in sr) are $F_\lambda = \Omega B_\lambda$, $F_\nu = \Omega B_\nu$, $F_\lambda = 3.0 \times 10^{14} F_\nu/\lambda^2_{\mu\text{m}}$. Other units are 1 Jansky (Jy) = 10^{-26} W m^{-2} Hz^{-1}. Units details are given in Table 7.1.

Table 7.1. *Units* [1–4].

Units	Radiometric name	Astronomical name
W	Flux	Luminosity
W m^{-2}	Irradiance; radiant exitance	Flux
W sr^{-1}	Intensity	...
W m^{-2} sr^{-1}	Radiance	Intensity
W m^{-2} μm^{-1}; W m^{-2} Hz^{-1}	Spectral irradiance	Flux density
W m^{-2} μm^{-1} sr^{-1}; W m^{-2} Hz^{-1} sr^{-1}	Spectral radiance	Surface brightness; specific intensity

References
1. Boyd, R.W. 1983, *Radiometry and the Detection of Optical Radiation* (Wiley, New York)
2. Dereniak, E.L., & Crowe, D.G. 1984, *Optical Radiation Detectors* (Wiley, New York)
3. Wolfe, W.L., & Zissis, G.J. 1985, *The Infrared Handbook*, rev. ed. (Office of Naval Research, Washington, DC)
4. Rieke, G.H. 1994, *Detection of Light; From the Ultraviolet to the Submillimeter* (Cambridge University Press, Cambridge)

7.2 ATMOSPHERIC TRANSMISSION

The major atmospheric absorbers and central wavelengths of absorption bands are H_2O (0.94, 1.13, 1.37, 1.87, 2.7, 3.2, 6.3, $\lambda > 16$ μm); CO_2 (2.0, 4.3, 15 μm); N_2O (4.5, 17 μm); CH_4 (3.3, 7.7 μm); O_3 (9.6 μm). See Figures 7.1 and 7.2.

For atmospheric transmission at airborne and balloon altitudes, see [6, 11]. For water-vapor measurements at observatory sites, see [12–14]. For atmospheric extinction, see [2, 15–17].

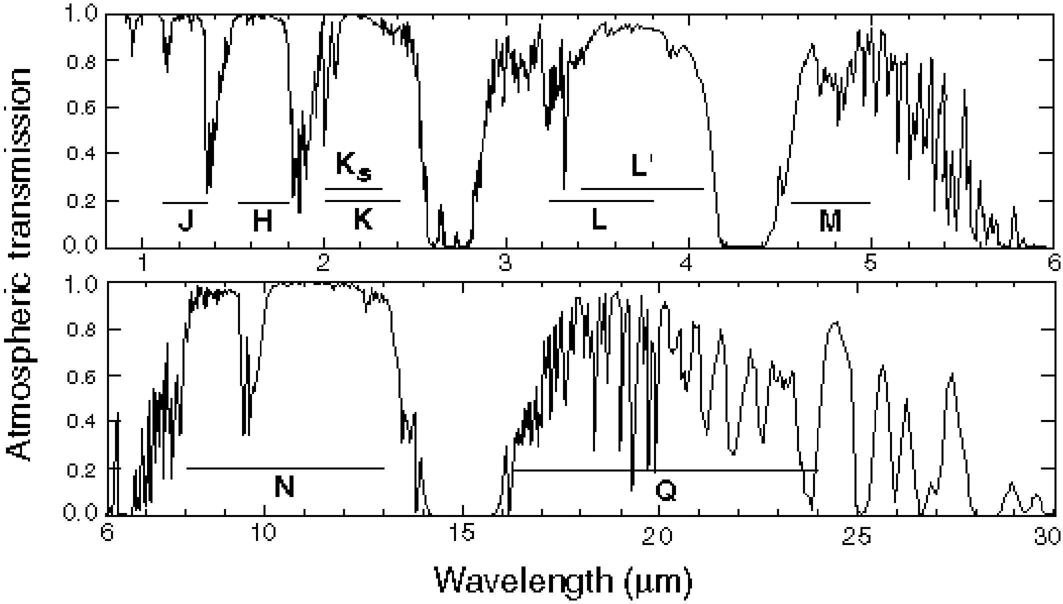

Figure 7.1. Atmospheric transmission from 0.9 to 30 μm under conditions appropriate for Mauna Kea, Hawaii. Altitude $=$ 4.2 km, zenith angle $=$ 30° (air mass $=$ 1.15), precipitable water vapor overhead $=$ 1 mm. $\lambda/\Delta\lambda = 300$ for 1–6 μm and 150 for 6–30 μm. Spectra are calculated by Lord [1]. The infrared filter band passes are shown as horizontal lines; see Table 7.5 for definitions. Note that the filter transmission is modified by the atmospheric absorption. For the atmospheric transmission at Kitt Peak, see [2]. For ESO, see [3]. See also [4].

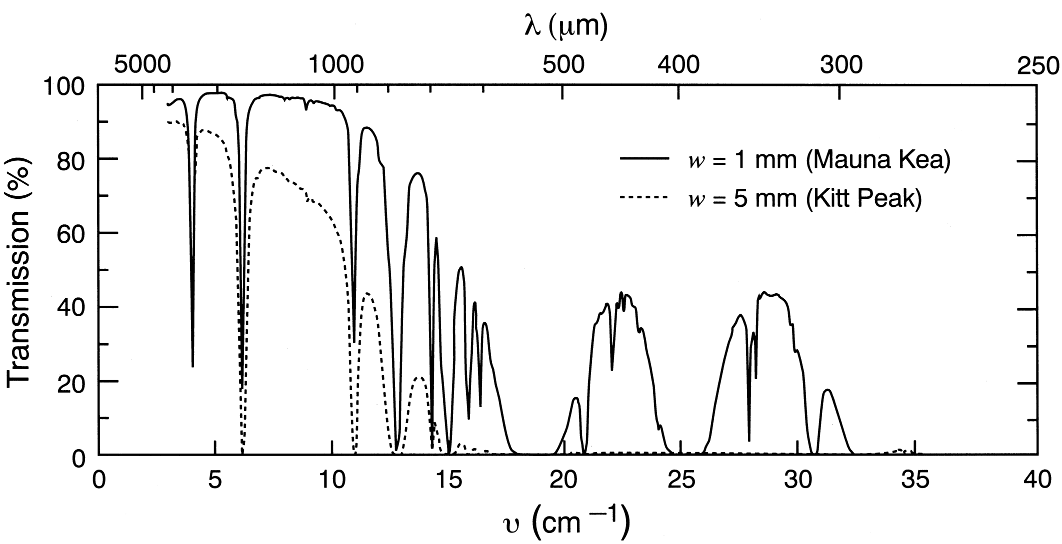

Figure 7.2. Atmospheric transmission from 0.25 to 3 mm, adapted from [5]. The precipitable water vapor is denoted by w. See also [6–9]. For the South Pole, see [10].

7.3 BACKGROUND EMISSION

7.3.1 Background Emission Sources

Table 7.2 gives the background emission from a ground-based telescope. The main background emission sources are shown in Figure 7.3. Where specified they are blackbody functions reduced by a multiplying factor ϵ. In most cases, only the minimum background levels are plotted.

OH OH airglow. Average OH emission of 15.6 and 13.8 mag arcsec^{-2} at J and H, respectively [18–21].
GBT Ground-based telescope thermal emission, optimized for the thermal infrared and approximated as a 273 K blackbody with $\epsilon = 0.02$. Emission from the Earth's atmosphere at 1.5–25 μm is shown [22].
ZSL Zodiacal scattered light at the ecliptic pole, approximated as a 5 800 K blackbody with $\epsilon = 3 \times 10^{-14}$ (based on data from [23]).
ZE Zodiacal emission from interplanetary dust at the ecliptic pole, approximated as a 275 K blackbody with $\epsilon = 7.1 \times 10^{-8}$. Based on observations from the Infrared Astronomical Satellite (IRAS) [24].
GBE Galactic background emission from interstellar dust in the plane of the Galaxy. In the plane of the Galaxy away from the Galactic Center, it can be approximated by a 17 K blackbody and $\epsilon = 10^{-3}$ [25, 26].
SEP South ecliptic pole emission as measured by the Cosmic Background Explorer (COBE) spacecraft [27].
CST Cryogenic space telescope, cooled to 10 K with $\epsilon = 0.05$.
CBR Cosmic background radiation, 2.73 K blackbody with $\epsilon = 1.0$ [28].

Table 7.2. *Combined sky, telescope, and instrument background emission at the* 3.0 m *IRTF* [1].[a]

Band	λ (μm)	$\Delta\lambda$	Surface brightness (mag arcsec^{-2})	Band	λ (μm)	$\Delta\lambda$	Surface brightness (mag arcsec^{-2})
J	1.26	0.31	15.9	L	3.50	0.61	4.9
H	1.62	0.28	13.4	L'	3.78	0.59	4.5
K_S	2.15	0.35	14.1	M'	4.78	0.22	0.3
K	2.21	0.39	13.7	M	4.85	0.62	−0.7

Note
[a] Telescope emissivity at the time of the observations was about 7%.

Reference
1. Shure, M. et al. 1994, *Proc. SPIE*, **2198**, 614

7.3.2 OH Emission Spectrum

The OH emission is often given in Rayleigh units. To convert to other units, use the following equations, with $\lambda_{\mu m}$ in μm [29]:

$$\begin{aligned} 1 \text{ Rayleigh unit} &= 10^{10}/4\pi \text{ photons s}^{-1}\,\text{m}^{-2}\,\text{sr}^{-1} \\ &= 1.5808 \times 10^{-10}/\lambda_{\mu m}\,\text{W}\,\text{m}^{-2}\,\text{sr}^{-1}, \end{aligned}$$

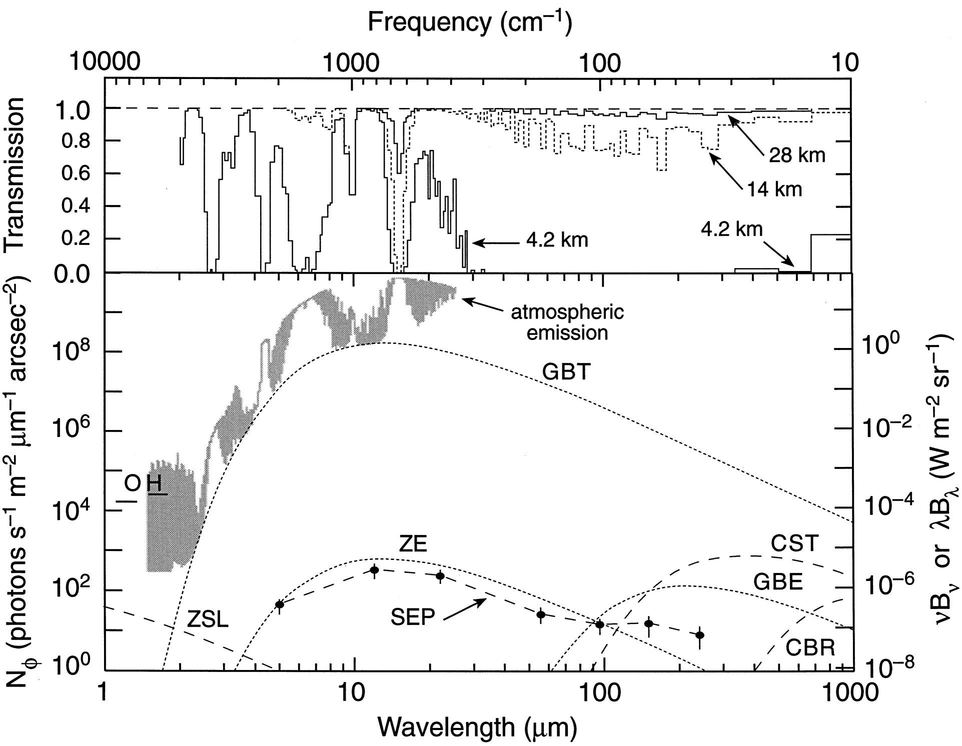

Figure 7.3. Top: Transmission of the Earth's atmosphere at Mauna Kea (4.2 km), airborne (14 km), and balloon altitudes (28 km), adapted from [6]. Bottom: Background emission sources. The surface brightness is calculated from $N_\phi = \epsilon\lambda_{\mu\mathrm{m}}B_\lambda/(hc) = 1.41 \times 10^{16}\,\epsilon\lambda_{\mu\mathrm{m}}^{-4}/(e^{14\,387.7/\lambda_{\mu\mathrm{m}}T} - 1)$ ($\lambda_{\mu\mathrm{m}}$ in μm, T in K). The intensity is derived from $\lambda_{\mu\mathrm{m}}B_\lambda = 8.45 \times 10^{-9}N_\phi$.

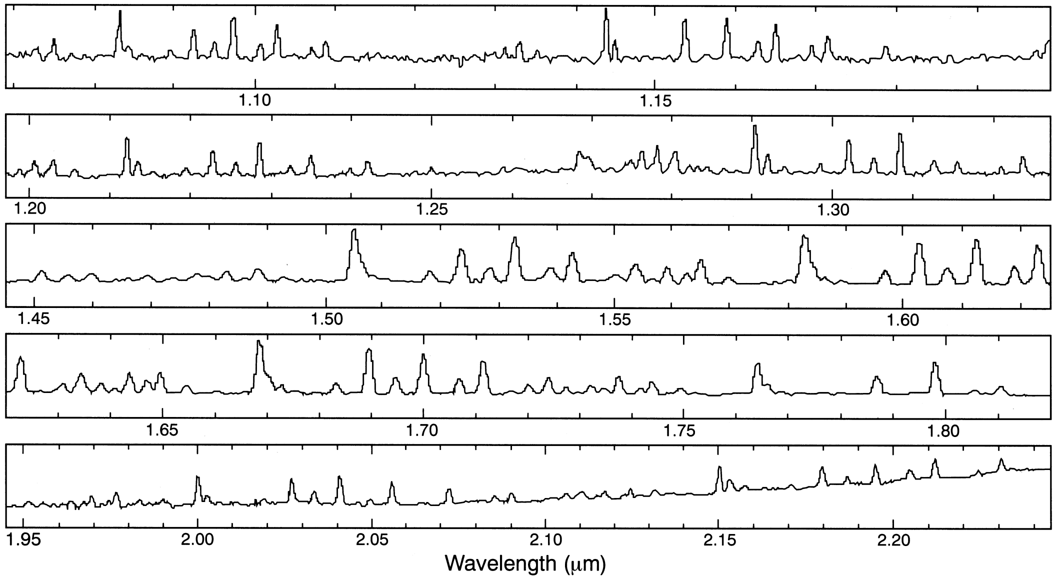

Figure 7.4. Observed OH airglow spectrum adapted from [30]. See also [19, 31–34, 29].

$$1 \text{ Rayleigh unit/Å} = 1.5808 \times 10^{-6}/\lambda_{\mu\text{m}} \text{ W m}^{-2}\,\mu\text{m}^{-1}\,\text{sr}^{-1}$$
$$= 3.7184 \times 10^{-17}/\lambda_{\mu\text{m}} \text{ W m}^{-2}\,\mu\text{m}^{-1}\,\text{arcsec}^{-2}.$$

The OH airglow spectrum is given in Figure 7.4.

7.4 DETECTORS AND SIGNAL-TO-NOISE RATIOS

Tables 7.3 and 7.4 list the basic detector types for infrared observations.

Table 7.3. *Basic detector types and typical useful wavelength ranges* [1–4].

Material	Type[a]	Wavelength range (μm)[b]	Material	Type[a]	Wavelength range (μm)[b]
Si	PD	< 1.1	Si:Sb	IBC	14–38
Ge	PD	< 1.8	Ge:Be	PC	30–50
HgCdTe	PD	1–2.5	Ge:Ga	PC	40–120
PtSi	SD	1–4	Ge:Ga	PC (stressed)	120–200
InSb	PD	1–5.6	Ge or Si	TD (bolometer)	200–1000
Si:As	IBC	6–27			

Notes

[a] PD = photodiode, PC = photoconductor, SD = Schottky diode, IBC = impurity band conduction photoconductor [also known as blocked impurity band (BIB) photoconductor]; TD = thermal detector.

[b] The HgCdTe long-wavelength cutoff is determined by the Hg/Cd ratio and can be extended to 25 μm.

References

1. Rieke, G.H. 1994, *Detection of Light: From the Ultraviolet to the Submillimeter* (Cambridge University Press, Cambridge)
2. Fazio, G.G. 1994, *Infrared Phys. Technol.*, **35**, 107
3. Herter, T. 1994, in *Infrared Astronomy with Arrays*, edited by I. McLean (Kluwer Academic, Dordrecht), p. 409
4. Haller, E.E. 1994, *Infrared Phys. Technol.*, **35**, 127

For an object that is distributed over n pixels, the signal photocurrent for photodiodes, photoconductors, and Schottky diodes is [35]

$$\sum_n i_s = A\tau\eta G\lambda F_\lambda \Delta\lambda/(hc) = A\tau\eta G(\Delta\lambda/\lambda)F_\nu/h \text{ electrons s}^{-1},$$

where i_s is the photocurrent from an individual pixel, A (m^2) is the telescope collecting area, τ is the transmission of instrument, telescope, and atmosphere, η is the detector quantum efficiency, G is the photoconductive gain ($=$ 1 for a photodiode; $\leq$ 0.5 for a photoconductor), $\Delta\lambda/\lambda$ is the fractional spectral bandwidth, F_λ (W m^{-2} μm^{-1}) $= \Omega_{\text{source}} B_\lambda$ = source flux density, and F_ν (W m^{-2} Hz^{-1}) $= \Omega_{\text{source}} B_\nu$ = source flux density.

The background photocurrent per pixel is

$$i_{\text{bg}} = A\tau\eta G N_\phi \Delta\lambda \Omega_{\text{pix}} \text{ electrons s}^{-1},$$

where N_ϕ (photons s^{-1} m^{-2} μm^{-1} arcsec^{-2}) is the background surface brightness and Ω_{pix} (arcsec^2) is the solid angle on the sky viewed by one pixel.

The RMS noise per pixel is

$$\left[N_r^2 + xG(i_s + i_{\rm bg} + i_{\rm dc})\,t\right]^{1/2}\ \text{electrons},$$

where N_r (electrons) is the detector read noise, $i_{\rm dc}$ (electrons s^{-1}) is the detector dark current, t (s) is the integration time, and $x = 1$ for a photodiode or IBC photoconductor or $x = 2$ for a photoconductor.

The signal-to-noise ratio before sky subtraction is

$$S/N = \left(\sum_n i_s\right) t \left(\sum_n [\,N_r^2 + xG(i_s + i_{\rm bg} + i_{\rm dc})t]\right)^{-1/2}.$$

An alternative signal-to-noise ratio equation including the noise introduced by sky subtraction is [36]:

$$S/N = N_{\rm obj}[N_{\rm obj} + n_{\rm pix}(1 + n_{\rm pix}/n_{\rm bg})(N_r^2 + N_{\rm bg} + N_{\rm dc} + N_{\rm dig}^2)]^{-1/2},$$

where $N_{\rm obj}$ is the total number of signal electrons from the object ($= \sum i_s\ t$), $n_{\rm pix}$ is the number of pixels summed for the object, $n_{\rm bg}$ is the number of pixels summed for the sky subtraction, N_r is the read noise in electrons per pixel, $N_{\rm bg}$ is the sky background in electrons per pixel ($= xGi_{\rm bg}t$), $N_{\rm dc}$ is the dark current in electrons per pixel ($= xGi_{\rm dc}t$), and $N_{\rm dig}$ is the digitization noise in electrons per pixel (usually negligible).

Table 7.4. *Far-infrared heterodyne detectors* [1,2].

Type	Wavelength range (μm)
Schottky diode	100–300
Superconducting–insulator–superconducting (SIS)	300–3000

References

1. Phillips, T.G. 1988, in *Millimetre and Submillimetre Astronomy*, edited by R.D. Wolstencroft and W.B. Burton (Kluwer Academic, Dordrecht), p. 1
2. White, G.J. 1988, in *Millimetre and Submillimetre Astronomy*, edited by R.D. Wolstencroft and W.B. Burton (Kluwer Academic, Dordrecht), p. 27

For a heterodyne receiver [37],

$$S/N = (T_S/T_N)\sqrt{t\,\Delta\nu},$$

where T_S is the source temperature (K), T_N is the equivalent Rayleigh–Jeans noise temperature (K) of the receiver, and $\Delta\nu$ (Hz) is the channel width of the radio integrator.

7.5 PHOTOMETRY ($\lambda < 30\ \mu$m)

There is no common infrared photometric (radiometric) system. As a result, filter central wavelengths, filter bandwidths, and instrumental responses are different at each observatory, as are the effects of the atmospheric transmission. The flux density of Vega established by Cohen et al. [38] is presented in Table 7.5. It is based upon an atmospheric model for Vega and the flux density calibration at 0.555 6 μm given by Hayes [39]. It is consistent with ground-based absolute flux density measurements to within $\leq 2\sigma$ of the measurement errors.

Table 7.5. *Filter wavelengths, bandwidths, and flux densities for Vega.*[a]

Filter name	$\lambda_{\rm iso}$[b] (μm)	$\Delta\lambda$[c] (μm)	F_λ (W m^{-2} μm^{-1})	F_ν (Jy)	N_ϕ (photons s^{-1} m^{-2} μm^{-1})
V	0.5556[d]	···	3.44×10^{-8}	3 540	9.60×10^{10}
J	1.215	0.26	3.31×10^{-9}	1 630	2.02×10^{10}
H	1.654	0.29	1.15×10^{-9}	1 050	9.56×10^{9}
K_S	2.157	0.32	4.30×10^{-10}	667	4.66×10^{9}
K	2.179	0.41	4.14×10^{-10}	655	4.53×10^{9}
L	3.547	0.57	6.59×10^{-11}	276	1.17×10^{9}
L'	3.761	0.65	5.26×10^{-11}	248	9.94×10^{8}
M	4.769	0.45	2.11×10^{-11}	160	5.06×10^{8}
8.7	8.756	1.2	1.96×10^{-12}	50.0	8.62×10^{7}
N	10.472	5.19	9.63×10^{-13}	35.2	5.07×10^{7}
11.7	11.653	1.2	6.31×10^{-13}	28.6	3.69×10^{7}
Q	20.130	7.8	7.18×10^{-14}	9.70	7.26×10^{6}

Notes

[a] Cohen et al. [1] recommend the use of Sirius rather than Vega as the photometric standard for $\lambda > 20$ μm because of the infrared excess of Vega at these wavelengths. The magnitude of Vega depends on the photometric system used, and it is either assumed to be 0.0 mag or assumed to be 0.02 or 0.03 mag for consistency with the visual magnitude.

[b] The infrared isophotal wavelengths and flux densities (except for K_S) are taken from Table 1 of [1], and they are based on the UKIRT filter set and the atmospheric absorption at Mauna Kea. See Table 2 of [1] for the case of the atmospheric absorption at Kitt Peak. The isophotal wavelength is defined by $F(\lambda_{\rm iso}) = \int F(\lambda)S(\lambda)\,d\lambda / \int S(\lambda)\,d\lambda$, where $F(\lambda)$ is the flux density of Vega and $S(\lambda)$ is the (detector quantum efficiency) $\times$ (filter transmission) $\times$ (optical efficiency) $\times$ (atmospheric transmission) [2]. $\lambda_{\rm iso}$ depends on the spectral shape of the source and a correction must be applied for broadband photometry of sources that deviate from the spectral shape of the standard star [3]. The flux density and $\lambda_{\rm iso}$ for K_S were calculated here. For another filter, K', at 2.11 μm, see [4].

[c] The filter full width at half maximum.

[d] The wavelength at V is a monochromatic wavelength; see [5].

References

1. Cohen, M. et al. 1992, *AJ*, **104**, 1650
2. Golay, M. 1974, *Introduction to Astronomical Photometry* (Reidel, Dordrecht), p. 40
3. Hanner, M.S., et al. 1984, *AJ*, **89**, 162
4. Wainscoat, R.J., & Cowie, L.L. 1992, *AJ*, **103**, 332
5. Hayes, D.S. 1985, in *Calibration of Fundamental Stellar Quantities*, edited by D.S. Hayes, et al., Proc. IAU Symp. No. 111 (Reidel, Dordrecht), p. 225

Absolute calibration. (a) For 1.2–5 μm, see [40]. (b) For 10–20 μm, see [41].

Photometric systems and standard star observations. For AAO, 1.2–3.8 μm, see [42]; for CIT, 1.2–3.5 μm, see [43]; for ESO, 1.2–3.8 μm, see [44]; for ESO, 1.2–4.8 μm, see [45]; for IRTF, 10–20 μm, see [46]; for KPNO, 1.2–2.2 μm, see [47]; for MSO, 1.2–2.2 μm, see [48]; for OAN, 1.2–2.2 μm, see [49]; for SAAO, 1.2–3.4 μm, see [50]; for UA, IRTF, WIRO, 1.2–20 μm, see [51]; for UKIRT, 1–2.2 μm, faint standards, see [52]; for WIRO, 1.2–33 μm, see [53].

Color transformations. For *JHKLL′M*; SAAO–Johnson, SAAO-ESO, SAAO–AAO, AAO–MSO, AAO–CIT, see [17]; for *JHKLM*; ESO–SAAO; ESO–AAO; ESO–MSSSO; ESO–CTIO, see [44]; for *JHK*; OAN–CIT, OAN–AAO, OAN–ESO, OAN–Johnson, see [49]; for *JHKL*; SAAO–ESO, SAAO–AAO, SAAO–MSSSO, SAAO–CTIO, see [50]; for *JHKL*; CIT–AAO, CIT–SAAO, CIT–Johnson, see [54]; for *JHKLM*; Johnson–ESO, Johnson–SAAO, see [55]; for *JHK*; CIT–IRTF, CIT–UKIRT, CIT–CTIO, CIT–ESO, CIT–KPNO, CIT–HCO, CIT–AAO, CIT–Johnson/Glass, see [56].

Acronyms. AAO = Anglo-Australian Observatory; CIT = California Institute of Technology; CTIO = Cerro Tololo Inter-American Observatory; ESO = European Southern Observatory; HCO =

Harvard College Observatory (Mt. Hopkins); IRTF = NASA Infrared Telescope Facility; KPNO = Kitt Peak National Observatory; MSO = Mt. Stromlo Observatory; MSSSO = Mt. Stromlo/Siding Springs Observatory; OAN = San Pedro Mártir National Observatory; SAAO = South African Astronomical Observatory; UA = University of Arizona; UKIRT = United Kingdom Infrared Telescope; WIRO = Wyoming Infrared Observatory.

Tables 7.6–7.8 give intrinsic colors and effective temperatures for stars.

Table 7.6. *Intrinsic colors and effective temperatures for the main sequence (class* V*).*[a]

Spectral type	$V-K$	$J-H$	$H-K$	$K-L$	$K-L'$	$K-M$	$T_{\rm eff}$[b]
O9	−0.87	−0.14	−0.04	−0.06			35 900
O9.5	−0.85	−0.13	−0.04	−0.06			34 600
B0	−0.83	−0.12	−0.04	−0.06			31 500
B1	−0.74	−0.10	−0.03	−0.05			25 600
B2	−0.66	−0.09	−0.03	−0.05			22 300
B3	−0.56	−0.08	−0.02	−0.05			19 000
B4	−0.49	−0.07	−0.02	−0.05			17 200
B5	−0.42	−0.06	−0.01	−0.04			15 400
B6	−0.36	−0.05	−0.01	−0.04			14 100
B7	−0.29	−0.03	−0.01	−0.04			13 000
B8	−0.24	−0.03	0.00	−0.04			11 800
B9	−0.13	−0.01	0.00	−0.03			10 700
A0	0.00	0.00	0.00	0.00	0.00	0.00	9 480
A2	0.14	0.02	0.01	0.01	0.01	0.01	8 810
A5	0.38	0.06	0.02	0.02	0.02	0.03	8 160
A7	0.50	0.09	0.03	0.03	0.03	0.03	7 930
F0	0.70	0.13	0.03	0.03	0.03	0.03	7 020
F2	0.82	0.17	0.04	0.03	0.03	0.03	6 750
F5	1.10	0.23	0.04	0.04	0.04	0.02	6 530
F7	1.32	0.29	0.05	0.04	0.04	0.02	6 240
G0	1.41	0.31	0.05	0.05	0.05	0.01	5 930
G2	1.46	0.32	0.05	0.05	0.05	0.01	5 830
G4	1.53	0.33	0.06	0.05	0.05	0.01	5 740
G6	1.64	0.37	0.06	0.05	0.05	0.00	5 620
K0	1.96	0.45	0.08	0.06	0.06	−0.01	5 240
K2	2.22	0.50	0.09	0.07	0.07	−0.02	5 010
K4	2.63	0.58	0.11	0.09	0.10	−0.04	4 560
K5	2.85	0.61	0.11	0.10	0.11		4 340
K7	3.16	0.66	0.15	0.11	0.13		4 040
M0	3.65	0.67	0.17	0.14	0.17		3 800
M1	3.87	0.66	0.18	0.15	0.21		3 680
M2	4.11	0.66	0.20	0.16	0.23		3 530
M3	4.65	0.64	0.23	0.20	0.32		3 380
M4	5.28	0.62	0.27	0.23	0.37		3 180
M5	6.17	0.62	0.33	0.29	0.42		3 030
M6	7.37	0.66	0.38	0.36	0.48		2 850

Notes

[a] Colors given in the Johnson–Glass system as established by Bessell and Brett [1]. References used: O, B, [2]; A, F, G, K, [1]; K, M, [3]. Did not use K–M from [2] because there is a large offset compared to [1]. Approximate uncertainties (one standard deviation): ±0.02 (O−K); ±0.03 (M).

[b] $T_{\rm eff}$ is an average of values from the following sources: for O, B, [4]; for B, A, F, G, K, [5]; for B, G, K, [6]; for A, F, [7]; for A, F, G, K, [8]; for A, F, G, [9]; for G, K, [10]; for K, M, [3]; for M, [11], [7], [12]. Approximate uncertainties (one standard deviation): ±1000 K (O9−B2); ±250 K (B3−B9); ±100 K (A0−M6).

References

1. Bessell, M.S., & Brett, J.M. 1988, *PASP*, **100**, 1134

2. Koornneef, J. 1983, *A&A*, **128**, 84
3. Bessell, M.S. 1991, *AJ*, **101**, 662
4. Vacca, W.D. et al. 1996, *ApJ*, **460**, 914
5. Popper, D.M. 1980, *ARA&A*, **18**, 115
6. Böhm-Vitense, E. 1981, *ARA&A*, **19**, 295
7. Böhm-Vitense, E. 1982, *ApJ*, **255**, 191
8. Blackwell, D.E. et al. 1991, *A&A*, **245**, 567
9. Fernley, J.A. 1989, *MNRAS*, **239**, 905
10. Bell, R.A., & Gustafsson, B. 1989, *MNRAS*, **236**, 653
11. Jones, H.R.A. et al. 1995, *MNRAS*, **277**, 767
12. Leggett, S.K. et al. 1996, *ApJS*, **104**, 117

Table 7.7. *Intrinsic colors and effective temperatures for giant stars (class* III*).*[a]

Spectral type	$V-K$	$J-H$	$H-K$	$K-L$	$K-L'$	$K-M$	$T_{\rm eff}$[b]
G0	1.75	0.37	0.07	0.04	0.05	0.00	5 910
G4	2.05	0.47	0.08	0.05	0.06	−0.01	5 190
G6	2.15	0.50	0.09	0.06	0.07	−0.02	5 050
G8	2.16	0.50	0.09	0.06	0.07	−0.02	4 960
K0	2.31	0.54	0.10	0.07	0.08	−0.03	4 810
K1	2.50	0.58	0.10	0.08	0.09	−0.04	4 610
K2	2.70	0.63	0.12	0.09	0.10	−0.05	4 500
K3	3.00	0.68	0.14	0.10	0.12	−0.06	4 320
K4	3.26	0.73	0.15	0.11	0.14	−0.07	4 080
K5	3.60	0.79	0.17	0.12	0.16	−0.08	3 980
M0	3.85	0.83	0.19	0.12	0.17	−0.09	3 820
M1	4.05	0.85	0.21	0.13	0.17	−0.10	3 780
M2	4.30	0.87	0.22	0.15	0.19	−0.12	3 710
M3	4.64	0.90	0.24	0.17	0.20	−0.13	3 630
M4	5.10	0.93	0.25	0.18	0.21	−0.14	3 560
M5	5.96	0.95	0.29	0.20	0.22	−0.15	3 420
M6	6.84	0.96	0.30				3 250
M7	7.80	0.96	0.31				

Notes

[a] Colors given in the Johnson–Glass system as established by Bessell and Brett in [1]. Approximate uncertainties (one standard deviation): ±0.02.

[b] $T_{\rm eff}$ is an average of values from the following sources: for G, K, M, [2]; for K, M, [3]; for G, K, [4]; for G, K, M, [5]. Approximate uncertainties (one standard deviation): ±50 K (G2−K5); ±70 K (M0–M6). For O and B stars, see [6].

References

1. Bessell, M.S., & Brett, J.M. 1988, *PASP*, **100**, 1134
2. Ridgway, S.T. et al. 1980, *ApJ*, **235**, 126
3. Di Benedetto, G.P., & Rabbia, Y. 1987, *A&A*, **188**, 114
4. Bell, R.A., & Gustafsson, B. 1989, *MNRAS*, **236**, 653
5. Blackwell, D.E. et al. 1991, *A&A*, **245**, 567
6. Vacca, W.D. et al. 1996, *ApJ*, **460**, 914

Table 7.8. *Intrinsic colors and effective temperatures for supergiant stars (class* I*).*[a]

Spectral type	$V-K$	$J-H$	$H-K$	$K-L$	$T_{\rm eff}$[b]
O9	−0.82	−0.05	−0.13	−0.08	32 500
B0	−0.69	−0.04	−0.10	−0.07	26 000
B1	−0.55	−0.03	−0.06	−0.07	20 700
B2	−0.40	−0.04	0.00	−0.07	17 800
B3	−0.28	−0.03	0.03	−0.05	15 600
B4	−0.20	−0.01	0.01	−0.01	13 900

Table 7.8. *(Continued.)*

Spectral type	$V-K$	$J-H$	$H-K$	$K-L$	$T_{\mathrm{eff}}{}^{b}$
B5	−0.13	0.01	0.00	0.02	13 400
B6	−0.07	0.04	−0.02	0.03	12 700
B7	0.01	0.06	−0.02	0.04	12 000
B8	0.07	0.07	−0.02	0.05	11 200
B9	0.13	0.08	−0.02	0.06	10 500
A0	0.19	0.09	−0.02	0.07	9 730
A1	0.26	0.11	−0.01	0.07	9 230
A2	0.32	0.12	−0.01	0.08	9 080
A5	0.48	0.13	0.02	0.07	8 510
F0	0.64	0.15	0.04	0.06	7 700
F2	0.75	0.18	0.05	0.06	7 170
F5	0.93	0.22	0.06	0.07	6 640
F8	1.21	0.28	0.07	0.07	6 100
G0	1.44	0.33	0.08	0.08	5 510
G3	1.67	0.38	0.09	0.08	4 980
G8	1.99	0.43	0.11	0.09	4 590
K0	2.15	0.46	0.12	0.10	4 420
K1	2.28	0.49	0.13	0.11	4 330
K2	2.43	0.52	0.13	0.12	4 260
K3 Iab	2.90	0.59	0.13	0.15	4 130
K5 Iab	3.50	0.67	0.14	0.18	3 850
M0 Iab	3.80	0.73	0.18	0.20	3 650
M1 Iab	3.90	0.73	0.20	0.22	3 550
M2 Iab	4.10	0.73	0.22	0.24	3 450
M3 Iab	4.60	0.74	0.24	0.26	3 200
M4 Iab	5.20	0.78	0.26	0.28	2 980
M0 Ib	3.80	0.76	0.18	0.12	
M1 Ib	3.90	0.76	0.20	0.14	
M2 Ib	4.10	0.76	0.22	0.16	
M3 Ib	4.60	0.77	0.24	0.18	
M4 Ib	5.20	0.81	0.26	0.20	
M0 Ia	3.80	0.61	0.18	0.27	
M1 Ia	3.90	0.61	0.20	0.29	
M2 Ia	4.10	0.61	0.22	0.31	
M3 Ia	4.60	0.62	0.24	0.33	
M4 Ia	5.20	0.66	0.26	0.35	

Notes

[a] Colors given in the Johnson–Glass system as established by Bessell and Brett [1]. References used: For O, A, [2]; for A, F, G, K, [3]; for K, M, [4]. Approximate uncertainties (one standard deviation): ±0.03.

[b] T_{eff} is an average of values from the following references: For O–M, [5]; for O–K, [6]; for O, B, [7]. Approximate uncertainties (one standard deviation): ±1000 K (O9–B2); ±250 K (B3–B9); ±200 K (A–M).

References

1. Bessell, M.S., & Brett, J.M. 1988, *PASP*, **100**, 1134
2. Whittet, D.C.B., & van Breda, I.G. 1980, *MNRAS*, **192**, 467
3. Koornneef, J. 1983, *A&A*, **128**, 84
4. Elias, J. et al. 1985, *ApJS*, **57**, 91
5. Schmidt-Kaler, Th. 1982, in *Landolt-Börnstein*, New Series, edited by K. Schaifer & H.H. Voigt (Springer-Verlag, Berlin), Vol. VI/2b, p. 451
6. Böhm-Vitense, E. 1981, *ARA&A*, **19**, 295
7. Remie, H., & Lamers, H.J.G.L.M. 1982, *A&A*, **105**, 85

7.6 PHOTOMETRY ($\lambda > 30\ \mu$m)

The primary flux density calibrator for ground-based submillimeter and millimeter observations is Mars [57]. The main secondary calibrators are Uranus [58, 59] and Jupiter [5, 59, 60]. Other secondary calibrators consist of astronomical sources [59, 61].

Instrument details for the IRAS satellite are given in Table 7.9.

Table 7.9. *Infrared Astronomical Satellite (IRAS) summary information.*[a]

Effective wavelength (μm)	12	25	60	100
Bandwidth (FWHM) (μm)	7.0	11.15	32.5	31.5
Typical detector field of view, (in scan) × (cross scan) (arcmin)	0.76 × 4.55	0.76 × 4.65	1.51 × 4.75	3.03 × 5.05
Point Source Catalog, with 2 coverages, 90% completeness limits (Jy)[b]	0.45	⋯	0.64	⋯
Faint Source Catalog median 90% completeness limits (Jy)[b]	0.18	0.29	0.26	⋯

Notes

[a] IRAS observations are sensitive to dust with $T > 25$ K. For IRAS catalogs, see [1, 2].

[b] Completeness limits vary according to the amount of sky coverage obtained.

References

1. Infrared Astronomical Satellite (IRAS) Catalogs and Atlases, 1988, ed. Joint IRAS Science Working Group (U.S. Government Printing Office, Washington, DC), Vols. 1–7
2. The Infrared Processing & Analysis Center (IPAC) WWW Home Page (http://www.ipac.caltech.edu/) has numerous databases and information on IRAS catalogs

The following formulas give the IRAS four-band and two-band fluxes. For galactic sources [62]

$$F_{\rm ir}(7-135\ \mu{\rm m}) = 1.0\times10^{-14}(20.653\,f_{12} + 7.538\,f_{25} + 4.578\,f_{60} + 1.762\,f_{100})\ {\rm W\,m^{-2}}.$$

For extragalactic sources [63, 64]

$$F_{\rm ir}(8-1\,000\ \mu{\rm m}) = 1.8\times10^{-14}(13.48\,f_{12} + 5.16\,f_{25} + 2.58\,f_{60} + f_{100})\ {\rm W\,m^{-2}},$$
$$F_{\rm fir}(43-123\ \mu{\rm m}) = 1.26\times10^{-14}(2.58\,f_{60} + f_{100})\ {\rm W\,m^{-2}},$$

where f_{12}, f_{25}, f_{60}, and f_{100} are the IRAS flux densities in Jy at 12, 25, 60, and 100 μm. These formulas are approximations based on assumptions about the intrinsic source spectrum and dust emissivity. It is recommended that the original references be consulted for details.

The luminosity (in solar luminosities) is

$$L_{\rm ir,fir} = 3.127\times10^{7}D^2F_{\rm ir,fir}L_\odot,$$

where D is in pc and $F_{\rm ir,fir}$ is in ${\rm W\,m^{-2}}$.

The far-infrared emission–radio emission correlation [65] is

$$q = \log\{[F_{\rm fir}/(3.75\times10^{12}\ {\rm Hz})]/f_{1.4\ {\rm GHz}}\} = 2.14,$$

where $f_{1.4\ {\rm GHz}}$ is the 1.4 GHz flux density in ${\rm W\,m^{-2}\,Hz^{-1}}$.

7.7 INFRARED LINE LIST

Table 7.10 presents data for a sample of infrared lines.

Table 7.10. *Selected infrared lines.*

λ (μm)[a]	ν (cm^{-1})[a]	Species	Transition[b]	Reference[c]
1.005 21	9 948.17	H I	$n = 7$–3 (Paδ)	[1, 2, 3]
1.012 64	9 875.18	He II	$n = 5$–4	[1, 3]
1.083 3	9 231.2	He I	$2p\,^3P^o$–$2s\,^3S$	[1, 3]
1.094 11	9 139.85	H I	$n = 6$–3 (Paγ)	[1, 2, 3]
1.112 86	8 985.84	Fe II	$b\,^4G_{5/2}$–$z\,^4F_{3/2}$	[4, 5, 6]
1.129 0	8 857.4	O I	$3d\,^3D^o$–$3p\,^3P$	[2, 3, 4]
1.162 96	8 598.75	He II	$n = 7$–5	[1, 3]
1.167 64	8 564.28	He II	$n = 11$–6	[1, 7]
1.252	7 987.0	[Si IX]	$^3P_1 - {}^3P_2$	[8, 9, 10, 11]
1.257 02	7 955.30	[Fe II]	$a\,^4D_{7/2}$–$a\,^6D_{9/2}$	[4, 5, 6]
1.282 16	7 799.34	H I	$n = 5$–3 (Paβ)	[1, 2, 3]
1.316 82	7 594.03	O I	$4s\,^3S^o$–$3p\,^3P$	[3, 6]
1.476 44	6 773.05	He II	$n = 9$–6	[1, 3]
1.526 47	6 551.08	H I	$n = 19$–4 (Br19)	[1, 2, 3]
1.588 48	6 295.29	H I	$n = 14$–4 (Br14)	[1, 2, 3]
1.611 37	6 205.92	H I	$n = 13$–4 (Br13)	[1, 2, 3]
1.618 9	6 177.0	CO	$v = 6$–3 band head	[12]
1.626 46	6 148.32	OH	$v = 2$–0 $P_{1d}(15)$	[12]
1.641 17	6 093.21	H I	$n = 12$–4 (Br12)	[1, 2, 3]
1.644 00	6 082.73	[Fe II]	$a\,^4D_{7/2}$–$a\,^4F_{9/2}$	[4, 5, 6]
1.681 11	5 948.45	H I	$n = 11$–4 (Br11)	[1, 2, 3]
1.687 78	5 924.94	Fe II	$c\,^4F_{9/2}$–$z\,^4F_{9/2}$	[4, 5, 6]
1.692 30	5 909.12	He II	$n = 12$–7	[1, 7]
1.700 76	5 879.74	He I	$4d\,^3D - 3p\,^3P^o$	[3, 6]
1.736 69	5 758.08	H I	$n = 10$–4 (Br10)	[1, 2, 3]
1.741 88	5 740.94	Fe II	$c\,^4F_{7/2}$–$z\,^4D_{7/2}$	[3, 6]
1.817 91	5 500.82	H I	$n = 9$–4 (Br9)	[1, 2, 3]
1.875 61	5 331.60	H I	$n = 4$–3 (Paα)	[2, 3]
1.945 09	5 141.15	H I	$n = 8$–4 (Brδ)	[1, 2, 3]
1.957 56	5 108.40	H_2	$v = 1$–0 S(3)	[13, 14]
1.963 4	5 093.2	[Si VI]	$^2P_{1/2}$–$^2P_{3/2}$	[9, 10, 15]
2.033 76	4 917.01	H_2	$v = 1$–0 S(2)	[14, 16]
2.040	4 902.0	[Al IX]	$^2P^o_{3/2}$–$^2P^o_{1/2}$	[9, 10]
2.040 65	4 900.39	$H_3{}^+$	$v = 2\nu_2(2)$–0; (4, 6, +2)–(3, 3)	[17]
2.058 69	4 857.45	He I	$2p\,^1P^o$–$2s\,^1S$	[3, 18]
2.060 59	4 852.99	Fe II	$c\,^4F_{5/2}$–$z\,^4F_{3/2}$	[5, 6, 18]
2.089 38	4 786.11	Fe II	$c\,^4F_{3/2}$–$z\,^4F_{3/2}$	[5, 6, 16]
2.093 26	4 777.23	$H_3{}^+$	$v = 2\nu_2(2)$–0; (7, 9, +2)–(6, 6)	[17]
2.112 7	4 733.4	He I	$4s\,^3S$–$3p\,^3P^o$	[3, 6]
2.121 83	4 712.91	H_2	$v = 1$–0 S(1)	[14, 16]
2.137 48	4 678.41	Mg II	$5p\,^2P^o_{3/2}$–$5s\,^2S_{1/2}$	[18]
2.143 80	4 664.61	Mg II	$5p\,^2P^o_{1/2}$–$5s\,^2S_{1/2}$	[18]
2.166 12	4 616.55	H I	$n = 7$–4 (Brγ)	[2, 3, 16]
2.189 11	4 568.07	He II	$n = 10$–7	[1, 7]
2.206 24	4 532.59	Na I	$4p\,^2P^o_{3/2}$–$4s\,^2S_{1/2}$	[16, 19, 20]
2.208 97	4 527.00	Na I	$4p\,^2P^o_{1/2}$–$4s\,^2S_{1/2}$	[16, 19, 20]
2.223 29	4 497.84	H_2	$v = 1$–0 S(0)	[14, 16]
2.247 72	4 448.96	H_2	$v = 2$–1 S(1)	[14, 16]
2.263 11	4 418.69	Ca I	$4f\,^3F^o_3$–$4d\,^3D_2$	[19]

Table 7.10. *(Continued.)*

λ (μm)[a]	ν (cm^{-1})[a]	Species	Transition[b]	Reference[c]
2.265 73	4 413.58	Ca I	$4f\,^3F^o_4$–$4d\,^3D_3$	[19]
2.293 53	4 360.09	CO	$v = 2$–0 band head	[16]
2.322 65	4 305.42	CO	$v = 3$–1 band head	[16]
2.343 27	4 267.54	CO	$v = 2$–0 R(1)	[21]
2.345 31	4 263.84	CO	$v = 2$–0 R(0)	[21]
2.349 50	4 256.22	CO	$v = 2$–0 P(1)	[21]
2.351 67	4 252.30	CO	$v = 2$–0 P(2)	[21]
2.352 46	4 250.87	CO	$v = 4$–2 band head	[16]
2.382 95	4 196.48	CO	$v = 5$–3 band head	[16]
2.406 59	4 155.25	H_2	$v = 1$–0 Q(1)	[13, 14]
2.413 44	4 143.47	H_2	$v = 1$–0 Q(2)	[13, 14]
2.423 73	4 125.87	H_2	$v = 1$–0 Q(3)	[13, 14]
2.483 3	4 026.9	[Si VII]	$^3P_1$–$^3P_2$	[9, 10, 15]
2.499 95	4 000.08	H_2	$v = 1$–0 Q(7)	[14, 22]
2.625 87	3 808.26	H I	$n = 6$–4 (Brβ)	[2, 22]
2.626 88	3 806.80	H_2	$v = 1$–0 O(2)	[14, 22]
3.0 279	3 302.6	[Mg VIII]	$^2P^o_{3/2}$–$^2P^o_{1/2}$	[8, 9, 10, 15]
3.039 20	3 290.34	H I	$n = 10$–5 (Pfϵ)	[2]
3.091 69	3 234.48	He II	$n = 7$–6	[3]
3.133	3 192.0	OH	$v = 1$–0, K=9 multiplet	[23]
3.296 99	3 033.07	H I	$n = 9$–5 (Pfδ)	[2, 24]
3.418 84	2 924.97	He II	$n = 25$–11	[3, 24]
3.484 01	2 870.26	He II	$n = 17$–10	[3, 24]
3.501 16	2 856.20	H I	$n = 24$–6 (Hu24)	[2, 24]
3.522 03	2 839.27	H I	$n = 23$–6 (Hu23)	[2, 24]
3.624 6	2 758.9	H_2	$v = 0$–0 S(15)	[25, 26]
3.645 92	2 742.79	H I	$n = 19$–6 (Hu19)	[2, 25]
3.661	2 731.0	[Al VI]	$^3P_1 - {}^3P_2$	[8–10]
3.692 63	2 708.10	H I	$n = 18$–6 (Hu18)	[2, 25]
3.724 0	2 685.3	H_2	$v = 0$–0 S(14)	[26]
3.740 56	2 673.40	H I	$n = 8$–5 (Pfγ)	[2]
3.807 41	2 626.46	H_2	$v = 1$–0 O(7)	[14, 27]
3.846 2	2 600.0	H_2	$v = 0$–0 S(13)	[26, 27]
3.935	2 541	[Si IX]	$^3P_1$–$^3P_0$	[9, 10, 15]
3.953 00	2 529.72	$H_3{}^+$	$v = \nu_2(1)$–0; (1, 0, −1)–(1, 0)	[28]
4.004 5	2 497.2	SiO	$v = 2 - 0$ band head	[29]
4.020 87	2 487.02	H I	$n = 14$–6 (Hu14)	[2, 16]
4.037 81	2 476.59	He I	$5f\,^3F^o$–$4d\,^3D$	[3, 30]
4.049 00	2 469.75	He I	$5g\,^1G$–$4f\,^1F^o$; $5g\,^3G$–$4f\,^3F^o$	[30]
4.052 26	2 467.76	H I	$n = 5$–4 (Brα)	[2, 16]
4.170 79	2 397.63	H I	$n = 13$–6	[2, 16]
4.649 31	2 150.86	CO	$v = 1$–0 R(1)	[31]
4.653 78	2 148.79	H I	$n = 7$–5 (Pfβ)	[2, 16]
4.657 48	2 147.08	CO	$v = 1$–0 R(0)	[31]
4.674 15	2 139.43	CO	$v = 1$–0 P(1)	[31]
4.682 62	2 135.55	CO	$v = 1$–0 P(2)	[31]
4.694 62	2 130.10	H_2	$v = 0$–0 S(9)	[14]
5.053 1	1 979.0	H_2	$v = 0$–0 S(8)	[14, 26]
6.634	1 507	[Ni II]	$a\,^2D_{3/2}$–$a\,^2D_{5/2}$	[32]
6.985	1 432	[Ar II]	$^2P^o_{1/2}$–$^2P^o_{3/2}$	[33]
7.642	1 309	[Ne VI]	$^2P_{3/2}$–$^2P_{1/2}$	[9, 10]
8.991 35	1 112.18	[Ar III]	$^3P_1$–$^3P_2$	[33, 34]
10.51	951.5	[S IV]	$^2P^o_{3/2}$–$^2P^o_{1/2}$	[33]
10.521	950.48	[Co II]	$a\,^3F_3$–$a\,^3F_4$	[11, 32]
12.278 6	814.425	H_2	$v = 0$–0 S(2)	[14]
12.372 0	808.283	H I	$n = 7$–6 (Huα)	[2]

Table 7.10. *(Continued.)*

λ (μm)[a]	ν (cm^{-1})[a]	Species	Transition[b]	Reference[c]
12.813 5	780.424	[Ne II]	$^2P^o_{1/2}$–$^2P^o_{3/2}$	[33, 34]
15.56	642.7	[Ne III]	$^3P_1$–$^3P_2$	[33]
17.034 8	587.032	H_2	$v = 0$–0 S(1)	[14]
18.713 0	534.387	[S III]	$^3P_2$–$^3P_1$	[34, 35]
24.315 8	411.256	[Ne V]	$^3P_1$–$^3P_0$	[34, 35]
25.87	386.5	[O IV]	$^2P_{3/2}$–$^2P_{1/2}$	[33]
28.218 8	354.374	H_2	$v = 0$–0 S(0)	[14]
33.482	298.67	[S III]	$^3P_1$–$^3P_0$	[35, 36]
51.816	192.99	[O III]	$^3P_2$–$^3P_1$	[33, 35]
57.317	174.47	[N III]	$^2P^o_{3/2}$–$^2P^o_{1/2}$	[33]
63.183 7	158.269	[O I]	$^3P_1$–$^3P_2$	[37]
77.059	129.77	CO	$J = 34$–33	[37]
88.355	113.18	[O III]	$^3P_1$–$^3P_0$	[33, 35]
119.23	83.872	OH	$^2\Pi_{3/2}$ $J = 5/2$–$3/2$	[37]
119.44	83.724	OH	$^2\Pi_{3/2}$ $J = 5/2$–$3/2$	[37]
121.898	82.035 8	[N II]	$^3P_2$–$^3P_1$	[33, 38]
124.65	80.225	NH_3	$K = 3$, $J = 4$–3, $a - s$	[37]
145.526	68.716 2	[O I]	$^3P_0$–$^3P_1$	[33]
157.741	63.395 1	[C II]	$^2P^o_{3/2}$–$^2P^o_{1/2}$	[33]
162.81	61.421	CO	$J = 16$–15	[37]
205.178	48.738 2	[N II]	$^3P_1$–$^3P_0$	[38]
370.415	26.996 7	[C I]	$^3P_2$–$^3P_1$	[33]
371.65	26.907	CO	$J = 7$–6	[39]
609.135	16.416 7	[C I]	$^3P_1$–$^3P_0$	[33]

Notes

[a] Vacuum wavelengths and frequencies are given.

[b] Transition shown is (upper level)–(lower level).

[c] Because of space limitations, only a few transitions of each species are shown; see references for additional lines. Wavelength and frequencies were calculated or obtained from primary references where possible. For additional information, see [40–45].

References

1. Treffers, R.R. et al. 1976, *ApJ*, **209**, 793
2. Moore, C.E. 1993, in *Tables of Spectra of Hydrogen, Carbon, Nitrogen, and Oxygen Atoms and Ions*, edited by J.W. Gallagher (CRC, Boca Raton, FL); van Hoof, P.A.M., private communication
3. Bashkin, S., & Stoner, J.O. 1975, *Atomic Energy Levels and Grotian Diagrams* (North-Holland, Amsterdam); van Hoof, P.A.M., private communication
4. Allen, D.A. et al. 1985, *ApJ*, **291**, 280
5. Johansson, S. 1978, *Phys. Scr.*, **18**, 217
6. Hamann, F. et al. 1994, *ApJ*, **422**, 626
7. Moore, C.E. 1971, *Atomic Energy Levels*, NSRDS-NBS Publication No. 35; van Hoof, P.A.M., private communication
8. Woodward, C.E. et al. 1995, *ApJ*, **438**, 921
9. Greenhouse, M.A. et al. 1993, *ApJS*, **88**, 23
10. Gehrz, R.D. 1988, *ARA&A*, **26**, 377
11. Roche, P.F. et al. 1993, *MNRAS*, **261**, 522
12. Hinkle, K.H. 1978, *ApJ*, **220**, 210
13. Gautier III, T.H. et al. 1976, *ApJ*, **207**, L129
14. Black, J.H., & van Dishoeck, E.F. 1987, *ApJ*, **322**, 412
15. Reconditi, M., & Oliva, E. 1993, *A&A*, **274**, 662; Oliva, E. et al. 1994, *A&A*, **288**, 457
16. Scoville, N. et al. 1983, *ApJ*, **275**, 201
17. Drossart, P. et al. 1989, *Nature*, **340**, 539; see also Kao, L. et al. 1991, *ApJS*, **77**, 317
18. Simon, M., & Cassar, L. 1984, *ApJ*, **283**, 179
19. Kleinman, S.G., & Hall, D.N.B. 1986, *ApJS*, **62**, 501

20. Martin, W.C., & Zalubas, R. 1981, *J. Phys. Chem. Ref. Data Ser.*, **10**, 153
21. Black, J.H., & Willner, S.P. 1984, *ApJ*, **279**, 673
22. Davis, D.S. et al. 1982, *ApJ*, **259**, 166
23. Beer, R. et al. 1972, *ApJ*, **172**, 89
24. Lowe, R.P. et al. 1991, *ApJ*, **368**, 195
25. Sanford, S.A. 1991, *ApJ*, **376**, 599
26. Knacke, R.F., & Young, E.T. 1981, *ApJ*, **249**, L65
27. Brand, P.W.J.L. et al. 1989, *MNRAS*, **236**, 929
28. Oka, T., & Geballe, T.R. 1990, *ApJ*, **351**, L53
29. Hinkle, K.H. et al. 1976, *ApJ*, **210**, L141
30. Hamann, F., & Simon, M. 1986, *ApJ*, **311**, 909
31. Guelachvili, G. 1979, *J. Mol. Spectrosc.*, **75**, 251; Mitchell, G.F. et al. 1989, *ApJ*, **341**, 1020
32. Wooden, D.H. et al. 1993, *ApJS*, **88**, 477
33. Genzel, R. 1988, in *Millimetre and Submillimetre Astronomy*, edited by R.D. Wolstencroft and W.B. Burton (Kluwer Academic, Dordrecht), p. 223
34. Kelly, D.M., & Lacy, J.H. 1995, *ApJ*, **454**, L161
35. Emery, R.J., & Kessler, M.F. 1984, in *Galactic and Extragalactic Infrared Spectroscopy*, edited by M.F. Kessler and J.P. Phillips (Reidel, Dordrecht), p. 289
36. Stacy, G.J. et al. 1993, *Proc. SPIE*, **1946**, 238
37. Watson, D.M. 1984, in *Galactic and Extragalactic Infrared Spectroscopy*, edited by M.F. Kessler and J.P. Phillips (Reidel, Dordrecht), p. 195; Townes, C.H., & Melnick, G. 1990, *PASP*, **102**, 357
38. Colgan, S.W.J. et al. 1993, *ApJ*, **413**, 237
39. Howe, J.E. et al. 1993, *ApJ*, **410**, 179
40. H: Wynn-Williams, C.G. 1984, in *Galactic and Extragalactic Infrared Spectroscopy*, edited by M.F. Kessler and J.P. Phillips (Reidel, Dordrecht), p. 133
41. H_2: Schwartz, R.D. et al. 1987, *ApJ*, **322**, 403; Black, J.H., & van Dishoeck, E.F. 1987, *ApJ*, **322**, 412
42. CO: Goorvitch, D. 1994, *ApJS*, **95**, 535
43. Solar atlases: Livingston, W., & Wallace, L. 1991, *An Atlas of the Solar Spectrum in the Infrared from* 1850 *to* 9000 cm^{-1} *(*1.1–5.4 μm*)*, NSO Technical Report No. 91-001 (NOAO, Tucson); Wallace, L., & Livingston, W. 1992, *An Atlas of a Dark Sunspot Umbral Spectrum from* 1970 *to* 8640 cm^{-1} (1.16–5.1 μm), NSO Technical Report No. 92-001 (NOAO, Tucson)
44. Infrared spectra: Jourdain de Muizon, M. et al. 1994, *Database of Astronomical Infrared Spectroscopic Observations* (University of Leiden, Leiden)
45. Infrared wavelength calibration: Outred, M. 1978, *J. Phys. Chem. Ref. Data Ser.*, **7**, 1; Rao, K.N. et al. 1966, *Wavelength Standards in the Infrared* (Academic Press, New York)

7.8 DUST

For the infrared interstellar reddening law, see [66–69].

The total to selective absorption ([66–68], for $R = A_V/\mathrm{E}(B-V) = 3.1$) is

$$A_V/\mathrm{E}(J-K) = 5.82 \pm 0.1, \qquad A_V/\mathrm{E}(H-K) = 15.3 \pm 0.6,$$
$$A_V/\mathrm{E}(V-K) = 1.13 \pm 0.03,$$
$$A_\lambda/\mathrm{E}(J-K) = 2.4(\lambda)^{-1.75} \quad (\text{for } 0.9 < \lambda < 6\ \mu\text{m}).$$

The color excess ratio [67] is

$$\mathrm{E}(J-H)/\mathrm{E}(H-K) = 1.70 \pm 0.05.$$

The ratio of visual extinction to silicate band optical depth (τ_{Si}) [68, 70, 71] is

$$A_V/\tau_{\mathrm{Si}} = 19 \pm 1 \quad (\text{local interstellar medium}),$$
$$A_V/\tau_{\mathrm{Si}} = 11 \pm 2 \quad (\text{Galactic Center region}).$$

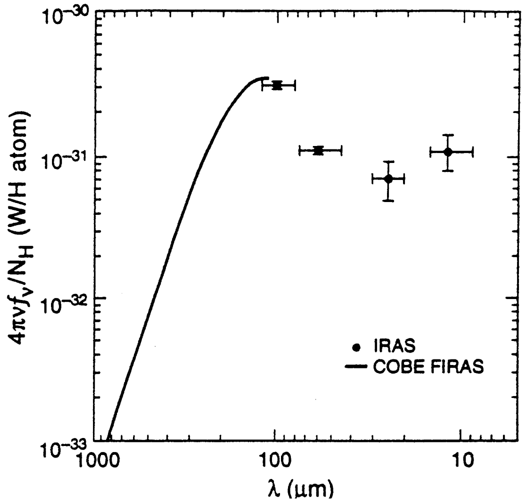

Figure 7.5. Emission spectrum of interstellar dust. Adapted from [78]. See also [26, 79, 80].

The average visual extinction to the Galactic Center region is 34 mag [72] and to individual sources it ranges from 23 to 35 mag [67].

The extinction cross section per H nucleus in the local interstellar medium [68] is

$$N_{\rm H}/{\rm E}(J-K) = 1.1\times 10^{22}\ \text{nuclei cm}^{-2}\,\text{mag}^{-1}.$$

The interstellar linear polarization [73–75]:

$$P(\lambda)/P_{\rm max} = \exp[-K\ln^2(\lambda_{\rm max}/\lambda)] \quad (\text{for } \lambda < 2\ \mu\text{m}),$$
$$P(\lambda) \propto \lambda^{-\beta}, \qquad \beta = 1.6 - 2.0 \quad (\text{for } 2 < \lambda < 5\ \mu\text{m}),$$

where $P(\lambda)$ is the percentage polarization, $P_{\rm max}$ is the maximum percentage polarization occurring at $\lambda_{\rm max}$, and $K = 0.01 \pm 0.05 + (1.66 \pm 0.09)\lambda_{\rm max}$.

Table 7.11 and Figure 7.5 present data on the interstellar dust emission. Table 7.12 presents far-infrared dust properties.

Table 7.11. *Average galactic diffuse emission* [1].[a]

λ (μm)	νI_ν (10^{-7} W m^{-2} sr^{-1})	λ (μm)	νI_ν (10^{-7} W m^{-2} sr^{-1})
3.5	0.21	60	0.88
4.9	0.13	100	2.0
12	0.80	140	3.8
25	0.41	240	2.5

Note

[a] For galactic latitudes −6° to −4° and +4° to +6°. Emission is highly variable on small spatial scales [1, 2].

References

1. Bernard, J.P. et al. 1994, *A&A*, **291**, L5
2. Cutri, R.M., & Latter, W.B., editors, 1993, *The First Symposium on the Infrared Cirrus and Diffuse Interstellar Clouds*, ASP Conf. Ser. (ASP, San Francisco), Vol. 58

The dust mass estimate from the 100 μm flux density is

$$M_{\text{dust}} = 4.81 \times 10^{-12} f_{100} D^2 (e^{143.88/T_d} - 1) \; M_\odot,$$

where f_{100} is the 100 μm flux density in Jy, D is the distance in pc, and T_d is the dust temperature in K. The derivation follows from [76], using a mass absorption coefficient of 2.5 $\text{m}^2\,\text{kg}^{-1}$ at 100 μm. The dust mass absorption coefficient at submillimeter wavelengths is estimated in [68, 76, 77].

The equilibrium dust temperature of a particle with albedo A at a distance r (in pc) from a source of luminosity L (in $L_\odot$) is

$$T_e = 0.612(1 - A)^{0.25} L^{0.25} r^{-0.5} \text{ K}.$$

The nonequilibrium emission from extremely small particles is discussed in [81–83].

Table 7.12. *Galactic dust properties at* 140–240 μm. *Mean values in the galactic plane* ($|b| < 1°$) [1].[a]

Quantity	Inner galaxy (270° < ℓ < 350°; 10° < ℓ < 90°)	Outer galaxy (90° < ℓ < 270°)	Entire galaxy
Dust temperature (K)	20 ± 1	17 ± 1	19 ± 1
240 μm optical depth	$(5.0 \pm 2.0) \times 10^{-3}$	$(9.5 \pm 3.0) \times 10^{-4}$	$(3.0 \pm 1.0) \times 10^{-3}$
Total FIR radiance ($\text{W m}^{-2}\,\text{sr}^{-1}$)	$(3.7 \pm 0.3) \times 10^{-5}$	$(2.4 \pm 0.2) \times 10^{-6}$	$(2.0 \pm 0.2) \times 10^{-5}$
Gas-to-dust ratio	140 ± 50	190 ± 60	160 ± 60
FIR luminosity per H mass ($L_\odot/\mathcal{M}_\odot$)	3.0 ± 0.3	0.9 ± 0.1	2.0 ± 0.2

Note

[a] Data from the Cosmic Background Explorer (COBE) satellite; for additional information, see the COBE WWW Home Page: http://www.gsfc.nasa.gov/astro/cobe/cobe_home.html

Reference

1. Sodroski, T.J. et al. 1994, *ApJ*, **428**, 638

Spectral features of dust and ice in the infrared are listed in Table 7.13.

Table 7.13. *Major dust and ice features* [1–7].

λ (μm)	Identification	Where observed
3.08	H_2O ice	Molecular clouds; OH–IR stars
3.29, 6.2, 7.7, 8.65, 11.25	Aromatic hydrocarbons[a]	H II regions, planetary nebulae, reflection nebulae, young and evolved stars, starburst galaxies
4.62	"X–CN"	Molecular clouds
4.67	CO ice	Molecular clouds
6.0	H_2O ice	Molecular clouds
6.85	CH_3OH + other	Molecular clouds
∼ 9.7	Amorphous silicates	H II regions, molecular clouds
∼ 11.2	SiC	Circumstellar shells; planetary nebulae
11.5	H_2O ice	OH–IR stars
∼ 18	Amorphous silicates	H II regions; Galactic center
∼ 34	MgS (?)	Planetary nebulae; carbon stars
43	H_2O ice	OH–IR stars

Note

[a] The nature of the "aromatic hydrocarbons" is not known precisely [7]; it is commonly assumed to be polycyclic aromatic hydrocarbons (PAHs).

References

1. Willner, S.P. 1984, in *Galactic and Extragalactic Infrared Spectroscopy*, edited by M.F. Kessler and J.P. Phillips (Reidel, Dordrecht), p. 37
2. Roche, P.F. 1989, in *Proc. 22nd ESLAB Symp. on Infrared Spectroscopy in Astronomy*, ESA SP-290, p. 79
3. Tokunaga, A.T., & Brooke, T.Y. 1990, *Icarus*, **86**, 208
4. Whittet, D.C.B. 1992, *Dust in the Galactic Environment* (Institute of Physics, Bristol), p. 147
5. Allamandola, L.J. et al. 1989, *ApJS*, **71**, 733
6. Léger, A., & d'Hendecourt, L. 1987, in *Polycyclic Aromatic Hydrocarbons and Astrophysics*, edited by A. Léger et al. (Reidel, Dordrecht), p. 223
7. Sellgren, K. 1994, in *The First Symposium on the Infrared Cirrus and Diffuse Interstellar Clouds*, edited by R.M. Cutri and W.B. Latter, ASP Conf. Ser. (ASP, San Francisco), Vol. 58, p. 243

7.9 SOLAR SYSTEM

The solar colors are [84]

$$J - H = 0.310, \quad H - K = 0.060, \quad K - L = 0.034, \quad L - M = -0.053, \quad V - K = 1.486.$$

Solar analogs [85] are 16 Cyg B, VB64, HD 105590, HR 2290.

The blackbody temperature of an object without an atmosphere in the solar system is

$$T_b = 278.8(1 - A)^{0.25} r^{-0.5} \text{ K},$$

where A is the albedo and r is the distance from the Sun in AU.

For thermal emission from asteroids, see [86–88].

For the infrared spectra of planetary atmospheres, see [89–92].

For the infrared spectra of comets, see [93, 94].

For near-infrared spectra of satellites, see [95, 96].

For near-infrared spectra of asteroids, see [97, 98].

The infrared magnitudes and colors of many solar system objects are given in Table 7.14.

Table 7.14. *Magnitudes of selected solar system bodies.*[a]

Object	Ref.	$V(1,0)^b$	ΔV^c	$V-J$	$J-H$	$H-K$	$K-L$	$V-N$	$V-Q$	T (K)^d
J1 Io	[1–4]	−1.68	0.15	1.3	0.35	0.08	0.00	4.70	9.29	137^e
J2 Europa (L)	[1–5]	−1.37	0.3	1.2	−0.31	−0.35	−2.24	3.91	8.81	130^e
J2 Europa (T)	[1–5]			1.4	−0.37	−0.53	−2.35			
J3 Ganymede (L)	[1–5]	−2.08	0.15	1.0	−0.10	−0.08	−1.90	5.69	10.26	142^e
J3 Ganymede (T)	[1–5]				−0.07	−0.07	−1.44			
J4 Callisto	[1–5]	−0.95	0.13	1.5	−0.27	0.07	−1.01	7.26	11.72	152^e
S2 Enceladus	[6–8]	1.9	0.5	1.06	−0.05	−0.24	< -0.5			
S3 Tethys	[4, 6, 7]	0.7	0.1	0.9	−0.20	−0.16				
S4 Dione	[4, 6, 7]	0.88	0.3	0.8	−0.20	−0.12				
S5 Rhea	[4, 5, 8, 9]	0.1	0.2	1.06	−0.05	−0.24	−1.6		8.5	
S6 Titan	[4, 10–13]	−1.3	0.0	0.2	−0.31	−0.38	−1.7	6.3		76^f
S8 Iapetus (L)	[13–15]	2.4		1.60	0.4	0.05				
S8 Iapetus (T)	[13–15]	0.6		0.8	−0.11	−0.13				
U1 Ariel	[4, 16]	1.7		1.20	0.21	−0.04				
U2 Umbriel	[7, 9]	2.4		1.30	0.25	−0.09			10.4	
U3 Titania	[4, 7, 9]	1.3		1.30	0.20	−0.14			10.0	
U4 Oberon	[7, 9]	1.6		1.35	0.20	−0.14			10.4	

Table 7.14. *(Continued.)*

Object	Ref.	$V(1,0)^b$	ΔV^c	$V-J$	$J-H$	$H-K$	$K-L$	$V-N$	$V-Q$	T (K)^d
N1 Triton	[5, 8, 17, 18]	−1.0		1.3	0.31	−0.24			> 8.2	38^d
Pluto, Charon	[17, 19–21]	−0.76	0.30	1.3	−0.01	−0.36			> 9.9	55^g
1 Ceres	[22–28]	3.72	0.04	1.2	0.31	0.05		10.0	12.8	245^h
2 Pallas	[22–28]	4.45	0.16	1.2	0.21	0.04		9.9	12.4	270^h
3 Juno	[22–28]	5.73	0.22			0.05		8.7	12.0	230^h
4 Vesta	[22–28]	3.55	0.12	1.4	0.17	0.01		8.4	11.2	250^h

Notes

[a] Average magnitude given unless indicated otherwise; (L) = leading hemisphere, (T) = trailing hemisphere. Approximate filter wavelengths: V (0.55 μm), J (1.25 μm), H (1.65 μm), K (2.2 μm), L (3.45 μm), N (10 μm), Q (20 μm); see references for details.

[b] $V(1,0)$ = absolute visual magnitude at a distance of 1 AU from the Earth and 1 AU from the Sun at 0° phase angle. The apparent visual magnitude of an object is $V(r,\Delta,\alpha) = V(1,0) + C\alpha + 5\log(r\Delta)$, where r is the heliocentric distance and Δ is the geocentric distance (both in AU), C is the phase coefficent in mag deg^{-1}, and α is the phase angle (deg). The opposition effect, occurring when $\alpha \approx 0°$, is not included in this table.

[c] ΔV = visual light curve amplitude (peak to peak).

[d] T_B = brightness temperature; T_S = surface or subsolar temperature.

[e] T_B (10 μm).

[f] T_B (100 μm).

[g] T_B (60 μm).

[h] T_S (10 μm).

References

1. Morrison, D. et al. 1976, *ApJ*, **207**, L213
2. Morrison, D. 1977, in *Planetary Satellites*, edited by J.A. Burns (University of Arizona, Tuscon), p. 269
3. Morrison, D., & Morrison, N.D. 1977, in *Planetary Satellites*, edited by J.A. Burns (University of Arizona, Tuscon), p. 363
4. Morrison, D., & Cruikshank, D.P. 1974, *SSRv*, **15**, 641
5. Hartmann, W.K. et al. 1982, *Icarus*, **52**, 377
6. Franz, O.G., & Millis, R.L. 1975, *Icarus*, **24**, 433
7. Cruikshank, D.P. 1980, *Icarus*, **41**, 246, and private communication
8. Cruikshank, D.P. et al. 1977, *ApJ*, **217**, 1006
9. Brown, R.H. et al. 1982, *Nature*, **300**, 423
10. Andersson, L.E. 1977, in *Planetary Satellites*, edited by J.A. Burns (University of Arizona, Tucson), p. 451
11. Noll, K.S., & Knacke, R.F. 1993, *Icarus*, **101**, 272
12. Gillett, F.C. 1975, *ApJ*, **201**, L41
13. Loewenstein, R.F. et al. 1980, *Icarus*, **43**, 283
14. Cruikshank, D.P. et al. 1983, *Icarus*, **53**, 90
15. Cruikshank, D.P. et al. 1979, *Rev. Geophys. Space Phys.*, **17**, 165
16. Nicholson, P.D., & Jones, T.J. 1980, *Icarus*, **42**, 54
17. Morrison, D. et al. 1982, *Nature*, **300**, 425
18. Tryka, K.A. et al. 1993, *Science*, **261**, 751
19. Binzel, R.P., & Mulholland, J.D. 1984, *AJ*, **89**, 1759
20. Soifer, B.T. et al. 1980, *AJ*, **85**, 166
21. Jewitt, D.C. 1994, *AJ*, **107**, 372
22. Veeder, G.J. et al. 1978, *AJ*, **83**, 651, and private communication
23. Lagerkvist, C.-I. et al. 1989, in *Asteroids* II, edited by R.P. Binzel et al. (University of Arizona, Tucson), p. 1162
24. Tedesco, E. 1979, in *Asteroids*, edited by T. Gehrels (University of Arizona, Tuscon), p. 1098
25. Johnson, T.V. et al. 1975, *ApJ*, **197**, 527
26. Morrison, D. 1974, *ApJ*, **194**, 203
27. Lebofsky, L.A. et al. 1986, *Icarus*, **68**, 239
28. McCheyne, R.S. et al. 1985, *Icarus*, **61**, 443

7.10 STARS

Molecular features seen in cool stars are listed in Table 7.15.

Table 7.15. *Molecular bands in cool stars* [1, 2].

Molecule	Bands	Wavelength range (μm)	Selected references
CO	$\Delta\nu = 1, 2, 3$	1.5–4.7	[3, 4, 5, 6, 7, 8, 9]
H_2	$\Delta\nu = 1$ (quadrapole vib-rot)	1.7–2.5	[3]
H_2O	$\nu_3, 2\nu_2, \nu_2 + \nu_3 - \nu_2, \nu_2 + \nu_3, \nu_1 + \nu_2$	1.3–3.6	[10, 11]
CN	$A\,^2\Pi – X\,^2\Sigma$	< 4	[3, 4, 6, 12, 13, 14, 15]
C_2	$b\,^1\Pi_u – x\,^1\Sigma_g^+$ (Phillips) $A'\,^3\Sigma_g^- – X'\,^3\Pi_u$ (Ballik–Ramsey)	< 2.5	[3, 6, 14, 16]
C_3, C_5	ν_3	4–5	[12, 17, 18]
HCN	$\nu_2, \nu_3, 2\nu_2, 3\nu_2, 2\nu_1 + \nu_2$	2–5, 7.1, 14	[13, 15, 16, 19]
C_2H_2	$\nu_3, \nu_5, \nu_1 + \nu_5$	2.5–4, 14	[13, 16, 19]
SiO	$\Delta\nu = 1, 2$	4–4.2, 8.0–8.3	[9, 20, 21, 22, 23]
OH	$\Delta\nu = 1, 2$	1.6–2.0, 3.1–4.0	[8, 22, 24]
CH	$\Delta\nu = 1$	3.3–4.0	[3, 22]
CS	$\Delta\nu = 2$	3.8–4.0	[22, 23]

References
1. Merrill, K.M., & Ridgway, S.T. 1979, *ARA&A*, **17**, 9
2. Tsuji, T. 1986, *ARA&A*, **24**, 89
3. Lambert, D.L. et al. 1986, *ApJS*, **62**, 373
4. Thompson, R.I. et al. 1972, *PASP*, **84**, 779
5. Ridgway, S.T. et al. 1974, in *Highlights of Astronomy*, edited by G. Contopoulos (Reidel, Dordrecht), Vol. 3, p. 327
6. Querci, M., & Querci, F. 1975, *A&A*, **42**, 329
7. Geballe, T.R. et al. 1977, *PASP*, **89**, 840
8. Hinkle, K.H. 1978, *ApJ*, **220**, 210
9. Cohen, M. et al. 1992, *AJ*, **104**, 2045
10. Strecker, D.W. et al. 1978, *AJ*, **83**, 26
11. Hinkle, K.H., & Barnes, T.G. 1979, *ApJ*, **227**, 923
12. Goebel, J.H. et al. 1978, *ApJ*, **222**, L129
13. Goebel, J.H. et al. 1981, *ApJ*, **246**, 455
14. Goebel, J.H. et al. 1983, *ApJ*, **270**, 190
15. Wiedemann, G.R. et al. 1991, *ApJ*, **282**, 321
16. Goebel, J.H. et al. 1980, *ApJ*, **235**, 104
17. Hinkle, K.H. et al. 1988, *Science*, **241**, 1319
18. Bernath, P.F. et al. 1989, *Science*, **244**, 562
19. Ridgway, S.T. et al. 1978, *ApJ*, **255**, 138
20. Geballe, T.R. et al. 1979, *ApJ*, **230**, L47
21. Rinsland, C.P., & Wing, R.F. 1982, *ApJ*, **262**, 201
22. Ridgway, S.T. et al. 1984, *ApJS*, **54**, 177
23. Lambert, D.L. et al. 1990, *AJ*, **99**, 1612
24. Beer, R. et al. 1972, *ApJ*, **172**, 89

For the spectrophotometry of standard stars, see [99–102].

For the infrared star count models, see [103–105].

Useful catalogs are found in [106–109].

For near-infrared spectra of young stars, see [110–118].

For spectral energy distributions of young stellar objects and pre–main sequence stars, see [119–124].

Figure 7.6 shows the color–color diagram for stars.

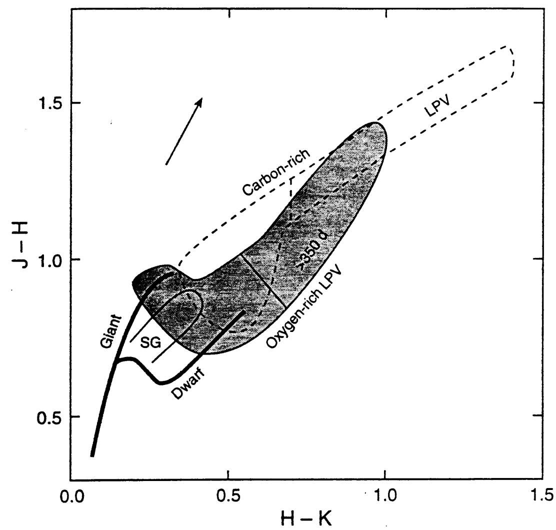

Figure 7.6. Color–color diagram for various classes of stars, adapted from [17]. The dark line indicates the location of G5 to M6 main sequence dwarf and giant stars. The dashed lines indicate the boundary for most carbon-rich stars; the carbon long-period variable (LPV) stars lie to the right. The oxygen-rich (M type) LPV stars fall within the boundary of the solid line, and the LPV stars with periods greater than 350 days are to the right and overlap the carbon-rich LPV stars. The supergiant M stars (SG) lie in a region below and to the right of the giant sequence. The arrow indicates the direction of the interstellar reddening.

7.11 EXTRAGALACTIC OBJECTS

7.11.1 Energy Distributions and Colors

Infrared energy distributions of galaxies vary widely. Representative examples may be found in [125, 126]. At least five different physical causes have been identified for the continuum infrared emission from galaxies:

(a) Photospheric emission from evolved stars (usually dominant in the 1–3 μm region) [127, 128]: Mean colors of elliptical galaxies (CIT photometric system): V–K = 3.33 mag; J–H = 0.69 mag; H–K = 0.21 mag. Molecular absorption bands in elliptical galaxies H_2O (1.95 μm) = 0.12 mag; CO (2.3 μm) = 0.16 mag. For additional near-infrared colors, see [129–132].

(b) Dust shells around evolved stars [133]: This is the main cause of 10–12 μm emission in elliptical galaxies, for which $f_\nu(12\ \mu\text{m}) = 0.13 f_\nu(2.2\ \mu\text{m})$. Units of f_ν are Jy.

(c) Emission from interstellar dust [134, 135]: Transiently heated "small" grains dominate at about 10 μm; "large" grains in thermal equilibrium dominate at 50–100 μm. A typical energy distribution from dust emission in a starburst galaxy normalized to 60 μm is $f_\nu(12\ \mu\text{m})$ = 0.035; $f_\nu(25\ \mu\text{m}) = 0.18$; $f_\nu(60\ \mu\text{m}) = 1.0$; $f_\nu(100\ \mu\text{m}) = 1.41$ [136].

(d) Seyfert nucleus: Seyfert galaxies exhibit infrared emission from dust heated by the central source, as well as emission from starburst or nonthermal components. Seyfert galaxies tend to be most prominent at 60 μm, but energy distributions vary widely. The IRAS 25–60 μm spectral slope has been found useful for selecting Seyfert galaxies [137, 138].

(e) Blazar component: Nonthermal, approximately power-law emission ($f_\nu \propto \nu^\alpha$). Mean values are $\alpha(1\ \mu\text{m}) = -1.42 \pm 0.95$; $\alpha(10\ \mu\text{m}) = -1.12 \pm 0.47$; $\alpha(100\ \mu\text{m}) = -0.88 \pm 0.43$; $\alpha(1\ \text{mm}) = -0.18 \pm 0.42$ [139].

For far-infrared colors of extragalactic objects, see [125, 140–143].

7.11.2 Statistics of Galaxies at Infrared Wavelengths

Galaxy number counts at 2.2 μm. The number of galaxies per square degree per magnitude is [144]:

$$dN/dK = 4\,000 \times 10^{\alpha(K-17)},$$

where α = 0.67 for $10 < K < 17$, α = 0.26 for $17 < K < 23$, and $K = 2.2\ \mu$m mag.

Luminosity function at 60 μm [125, 145]. The density of galaxies per cubic megaparsec per magnitude interval at 60 μm is

$$\log(\rho) = -3.2 - \alpha\,\{\log[\nu L_\nu(60\,\mu\mathrm{m})] - 10.2\}\,,$$

where $\nu L_\nu(60\ \mu\mathrm{m})$ is given in units of $L_\odot$, and $\alpha = 0.8$ for $\log[\nu L_\nu(60\ \mu\mathrm{m})] < 10.2$ and $\alpha = 2.0$ for $\log[\nu L_\nu(60\ \mu\mathrm{m})] > 10.2$. H_0 is assumed to be 75 km s^{-1} Mpc^{-1}.

The total infrared energy output of the local universe from 8 to 1000 μm is $1.24 \times 10^8 L_\odot$ Mpc^{-3} [146].

ACKNOWLEDGMENTS

Many people have helped with their comments and suggestions. I thank in particular the following persons for valuable comments and contributions to this chapter: E. Becklin, M. Cohen, D. Cruikshank, M. Hanner, T. Herter, J. Hora, E. Hu, T. Geballe, I. Glass, R. Knacke, S. Leggett, P. Léna, C. Lonsdale, S. Lord, J. Mazzarella, J. Pipher, S. Ridgway, K. Robertson, P. Roche, K. Sellgren, M. Simon, G. Veeder, M. Werner, G. Wynn-Williams, W. Vacca, and D. Van Buren.

REFERENCES

1. Lord, S. 1992, NASA Tech. Mem. 103957
2. Manduca, A., & Bell, R.A. 1979, *PASP*, **91**, 858
3. Bersanelli, M. et al. 1991, *A&A*, **252**, 854
4. Wolfe, W.L., & Zissis, G.J. 1985, *The Infrared Handbook*, rev. ed. (U.S. Government Printing Office, Washington, DC), p. 5-1
5. Griffin, M.J. et al. 1986, *Icarus*, **65**, 244
6. Traub, W.A., & Stier, M.T. 1976, *Appl. Opt.*, **15**, 364
7. Taylor, D.A. et al. 1991, *MNRAS*, **251**, 199
8. Taylor, D.A. et al. 1994, *Proc. SPIE*, **2198**, 703
9. Melnick, G.J. 1993, *Adv. Space Res.*, **13**, 535
10. Bally, J. 1989, in *Astrophysics in Antarctica*, AIP Conf. No. 198 (AIP, New York), p. 100; Townes, C.H., & Melnick, G. 1990, *PASP*, **102**, 357
11. Buhl, D. 1984, in *Galactic and Extragalactic Infrared Spectroscopy*, edited by M.F. Kessler and J.P. Phillips (Reidel, Dordrecht), p. 221
12. Warner, J.W. 1977, *PASP*, **89**, 724
13. Beckers, J.M. 1979, *PASP*, **91**, 857
14. Wallace, L. 1984, *PASP*, **96**, 184 & 836
15. Krisciunas, K. et al. 1987, *PASP*, **99**, 887
16. Volk, K. et al. 1989, in *Lecture Notes in Physics*, Vol. 341, edited by E.F. Milone (Springer-Verlag, Berlin), p. 15
17. Bessell, M.S., & Brett, J.M. 1988, *PASP*, **100**, 1134
18. Hodapp, K.-W. et al. 1992, *PASP*, **104**, 441
19. Maihara, T. et al. 1993, *PASP*, **105**, 940
20. Shure, M. et al. 1994, *Proc. SPIE*, **2198**, 614
21. Becklin, E., private communication
22. Roche, P.F., & Glasse, A.C.H. 1990, United Kingdom Large Telescope Report
23. Binzel, R.P. et al., this volume
24. Hauser, M.G. et al. 1984, *ApJ*, **278**, L15
25. Sodroski, T.J. et al. 1994, *ApJ*, **428**, 638
26. Cox, P., & Mezger, P.G. 1989, *A&A Rev.*, **1**, 49
27. Wright, E.L. 1993, *SPIE*, **2019**, 158
28. Mather, J.C. et al. 1994, *ApJ*, **420**, 439
29. Baker, D.J., & Romick, G.J. 1976, *Appl. Opt.*, **15**, 1966
30. Oliva, E., & Origlia, L. 1992, *A&A*, **254**, 466
31. Steed, A.J., & Baker, D.J. 1979, *Appl. Opt.*, **18**, 3386
32. McCaughrean, M.J. 1988, Ph.D. thesis, University of Edinburgh, Edinburgh
33. Ramsay, S.K. et al. 1992, *MNRAS*, **259**, 751
34. Osterbrock, D.E., & Martel, A. 1992, *PASP*, **104**, 76
35. Gillett, F.C. 1987, in *Infrared Astronomy with Arrays*, edited by C.G. Wynn-Williams and E.E. Becklin (University of Hawaii, Honolulu), p. 3
36. Merline, W.J., & Howell, S.B. 1995, *Exp. Astron.*, **6**, 163
37. Phillips, T.G. 1988, in *Millimeter and Submillimeter Astronomy*, edited by R.D. Wolstencroft and W.B. Burton (Kluwer Academic, Dordrecht), p. 1
38. Cohen, M. et al. 1992, *AJ*, **104**, 1650

39. Hayes, D.S. 1985, in *Calibration of Fundamental Stellar Quantities*, edited by D.S. Hayes et al., Proc. IAU Symp. No. 111 (Reidel, Dordrecht), p. 225
40. Blackwell, D.A. et al. 1990, *A&A*, **232**, 396; 1991, ibid., **245**, 567; Campins, H. et al. 1985, *AJ*, **90**, 896; Mountain, C.M. et al. 1985, *A&A*, **151**, 399
41. Rieke, G.H. et al. 1985, *AJ*, **90**, 900
42. Allen, D.A., & Cragg, T.A. 1983, *MNRAS*, **203**, 777
43. Elias, J.H. et al. 1982, *AJ*, **87**, 1029
44. Bersanelli, M. et al. 1991, *A&A*, **252**, 854
45. Bouchet, P. et al. 1991, *A&AS*, **91**, 409
46. Tokunaga, A.T. 1984, *AJ*, **89**, 172
47. Caillault, J.-P., & Patterson, J. 1990, *AJ*, **100**, 825
48. Jones, T.J., & Hyland, A.R. 1982, *MNRAS*, **200**, 509
49. Carrasco, L. et al. 1991, *PASP*, **103**, 987
50. Carter, B.S. 1990, *MNRAS*, **242**, 1
51. Hanner, M.S., & Tokunaga, A.T. 1991, in *Comets in the Post-Halley Era*, edited by R.L. Newburn et al. (Kluwer Academic, Dordrecht), p. 67
52. Casali, M., & Hawardsen, T. 1992, JCMT-UKIRT Newsletter, No. 4, p. 33
53. Gehrz, R.D. et al. 1987, in *Encyclopedia of Physical Science and Technology*, edited by R.A. Meyers (Academic Press, Orlando), Vol. 2, p. 53
54. Elias, J. et al. 1985, *ApJS*, **57**, 91
55. Koornneef, J. 1983, *A&AS*, **51**, 489
56. Leggett, S.K. et al. 1993, *IAU Colloq.*, **136**, 66
57. Wright, E.L. 1976, *ApJ*, **210**, 250
58. Orton, G.S. et al. 1986, *Icarus*, **67**, 289
59. Ulrich, B.L. 1981, *AJ*, **86**, 1619
60. Hildebrand, R.H. et al. 1985, *Icarus*, **64**, 64
61. Sandell, G. 1994, *MNRAS*, **271**, 75
62. Emerson, J.P. 1988, in *Formation and Evolution of Low Mass Stars*, edited by A.K. Dupree and M.T.V.T. Lago (Kluwer Academic, Dordrecht), Vol. 241, p. 193
63. Helou, G. et al. 1988, *ApJS*, **68**, 151
64. Pérault, M. 1987, Ph.D. thesis, University of Paris, Paris; Lonsdale, C., & Mazzarella, J., private communication
65. Helou, G. et al. 1985, *ApJ*, **298**, L7
66. Mathis, J.S., this volume
67. Rieke, G.H., & Lebofsky, M.J. 1985, *ApJ*, **288**, 618
68. Draine, B.T. 1989, in *Proceedings of the* 22*nd ESLAB Symposium on Infrared Spectroscopy in Astronomy*, edited by B.H. Kaldeich (ESA, Noordwijk), ESA SP-290, p. 93
69. He, L. et al. 1995, *ApJS*, **101**, 335
70. Roche, P.F., & Aitken, D.K. 1984, *MNRAS*, **208**, 481
71. Roche, P.F., & Aitken, D.K. 1985, *MNRAS*, **215**, 425
72. Henry, J.P. et al. 1984, *ApJ*, **285**, L27
73. Nagata, T. et al. 1994, *ApJ*, **423**, L113
74. Martin, P.G. et al. 1992, *ApJ*, **392**, 691
75. Whittet, D.C.B. et al. 1992, *ApJ*, **386**, 562
76. Hildebrand, R.H. et al. 1983, *QJRAS*, **24**, 267
77. Beckwith, S.V.W., & Sargent, A.I. 1991, *ApJ*, **381**, 250
78. Draine, B.T. 1994, in *First Symposium on the Infrared Cirrus and Diffuse Interstellar Clouds*, ASP Conf. Ser. Vol. 58, edited by R.M. Cutri and W.B. Latter (ASP, San Francisco), p. 227
79. Désert, F.X. et al. 1990, *A&A*, **237**, 215
80. Beichman, C.A. 1987, *ARA&A*, **25**, 521
81. Sellgren, K. 1984, *ApJ*, **277**, 623
82. Léger, A., & Puget, J.L. 1984, *A&A*, **137**, L5
83. Draine, B.T., & Anderson, N. 1985, *ApJ*, **292**, 494
84. Campins, H. et al. 1985, *AJ*, **90**, 896
85. Hardorp, J. 1982, *A&A*, **105**, 120
86. Lebofsky, L.A. et al. 1986, *Icarus*, **68**, 239
87. Morrison, D. 1974, *ApJ*, **194**, 203
88. Tedesco, E.F. et al. 1992, *The IRAS Minor Planet Survey*, Phillips Laboratory Report No. PL-TR-92-2049
89. Hanel, R.A. et al. 1992, *Exploration of the Solar System by Infrared Remote Sensing* (Cambridge University Press, Cambridge)
90. Encrenaz, Th., & Bibring, J.P. 1990, *The Solar System* (Springer-Verlag, Berlin)
91. Encrenaz, Th. 1992, in *Infrared Astronomy with ISO*, edited by Th. Encrenaz and M.F. Kessler (Nova Science, Commack), p. 173
92. Larson, H.P. 1980, *ARA&A*, **18**, 43
93. Crovisier, J. 1992, in *Infrared Astronomy with ISO*, edited by Th. Encrenaz and M.F. Kessler (Nova Science, Commack), p. 221
94. Mumma, M.J. et al. 1993, in *Protostars and Planets* III, edited by E.H. Levy and J.I. Lunine (University of Arizona, Tucson), p. 1177
95. Clark, R.N. et al. 1986, in *Satellites*, edited by J.A. Burns and M.S. Matthews (University of Arizona, Tucson), p. 437
96. Cruikshank, D.P., & Brown, R.H., in *Satellites*, edited by J.A. Burns and M.S. Matthews (University of Arizona, Tucson), p. 836
97. Larson, H.P., & Veeder, G.J. 1979, in *Asteroids* (University of Arizona, Tucson), p. 724
98. Gaffey, M.F. et al. 1989, in *Asteroids* II, edited by R.P. Binzel et al. (University of Arizona, Tucson), p. 98
99. Merrill, K.M., & Stein, W.A. 1976, *PASP*, **88**, 285
100. Strecker, D.W. et al. 1979, *ApJS*, **41**, 501
101. Cohen, M. et al. 1992, *AJ*, **104**, 2030
102. Walker, R.G., & Cohen, M. 1992, *An Atlas of Selected Calibrated Stellar Spectra*, NASA Contractor Report No. 177604
103. Wainscoat, R.J. et al. 1992, *ApJS*, **83**, 111
104. Cohen, M. 1993, *AJ*, **105**, 1860
105. Cohen, M. 1994, *AJ*, **107**, 582
106. Gezari, D.Y. et al. 1993, *Catalog of Infrared Observations*, 3rd ed. NASA Reference Publication No. 1294
107. Gezari, D.Y. et al. 1993, *Far Infrared Supplement, Catalog of Infrared Observations* ($\lambda > 4.6\ \mu$m), 3rd ed., Rev. 1, NASA Reference Publication No. 1295
108. Jourdain de Muizon, M. et al. 1994, *Database of Astronomical Infrared Spectroscopic Observations* (Leiden University, Leiden)
109. Kleinmann, S.G., & Hall, D.N.B. 1986, *ApJS*, **62**, 501
110. Scoville, N.Z. et al. 1983, *ApJ*, **275**, 201
111. Simon, M., & Cassar, L. 1984, *ApJ*, **283**, 179
112. Persson, S.E. et al. 1984, *ApJ*, **286**, 289
113. Hamann, F., & Simon, M. 1986, *ApJ*, **311**, 909
114. Schwartz, R.D. et al. 1987, *ApJ*, **322**, 403
115. Carr, J.S. 1989, *ApJ*, **345**, 522
116. Mitchell, G.F. et al. 1990, *ApJ*, **363**, 554
117. Chandler, C.J. et al. 1993, *ApJ*, **412**, L71

118. Hamann, F. et al. 1994, *ApJ*, **422**, 626
119. Lada, C.J. 1988, in *Formation and Evolution of Low Mass Stars*, edited by A.K. Dupree and M.T.V.T. Lago (Kluwer Academic, Dordrecht), p. 93
120. Shu, F.H. et al. 1987, *ARA&A*, **25**, 23
121. Wilking, B.A. 1989, *PASP*, **101**, 229
122. Lada, E.A. et al. 1993, in *Protostars and Protoplanets* III, edited by E.H. Levy and J.I. Lunine (University of Arizona, Tucson), p. 245
123. Zinnecker, H. et al. 1993, in *Protostars and Protoplanets* III, edited by E.H. Levy and J.I. Lunine (University of Arizona, Tucson), p. 429
124. André, P., & Montmerle, T. 1994, *ApJ*, **420**, 837
125. Soifer, B.T. et al. 1987, *ARA&A*, **25**, 187
126. Telesco, C.M. 1988, *ARA&A*, **26**, 343
127. Frogel, J.A. et al. 1978, *ApJ*, **220**, 75
128. Aaronson, M. et al. 1978, *ApJ*, **220**, 442
129. Glass, I.S. 1984, *MNRAS*, **211**, 461
130. Glass, I.S., & Moorwood, A.F.M. 1985, *MNRAS*, **214**, 429
131. Sanders, D.B. et al. 1988, *ApJ*, **325**, 74
132. Carico, D.P. et al. 1988, *AJ*, **95**, 356
133. Knapp, G.R. et al. 1992, *ApJ*, **399**, 76
134. Désert, F.X. et al. 1990, *A&A*, **237**, 215
135. Knapp, G.R. 1995, in *Airborne Astronomy Symposium on the Galactic Ecosystem: From Gas to Stars to Dust*, edited by M.R. Haas et al., ASP Conf. Ser. No. 73, p. 121
136. Roche, P.F. et al. 1991, *MNRAS*, **248**, 606
137. de Grijp, M.H.K. et al. 1985, *Nature*, **314**, 240
138. Glass, I.S. 1985, *MNASSA*, **44**, 60
139. Impey, C.D., & Neugebauer, G. 1988, *AJ*, **95**, 307
140. Soifer, B.T. et al. 1989, *AJ*, **98**, 766
141. Mazzarella, J.M. et al. 1991, *AJ*, **101**, 2034
142. Cohen, M. 1992, *AJ*, **103**, 1734
143. Walker, H.J. et al. 1989, *AJ*, **98**, 2163
144. Gardner, J.P. et al. 1993, *ApJ*, **415**, L9
145. Soifer, B.T. et al. 1987, *ApJ*, **320**, 238
146. Soifer, B.T., & Neugebauer, G. 1991, *AJ*, **101**, 354